Applied Soil Ecology 155 (2020) 103664

Contents lists available at ScienceDirect

Applied Soil Ecology

journal homepage: www.elsevier.com/locate/apsoil

Soil texture and straw type modulate the chemical structure of residues during four-year decomposition by regulating bacterial and fungal communities

Dandan Li[a,b], Bingzi Zhao[a,*], Dan C. Olk[c], Jiabao Zhang[a,*]

[a] State Key Laboratory of Soil and Sustainable Agriculture, Institute of Soil Science, Chinese Academy of Sciences, Nanjing 210008, China
[b] University of Chinese Academy of Sciences, Beijing 100049, China
[c] USDA-ARS, National Laboratory for Agriculture and the Environment, Ames, IA 50011, USA

ARTICLE INFO

Keywords:
Soil texture
Straw type
Bacterial and fungal community composition
Chemical structure

ABSTRACT

The changes of chemical structure and decomposer community during straw degradation have been inconsistent in previous reports, showing either convergence or divergence of chemical structures or microbial communities among different straw types. Hence the strength of their relationship remains unclear. Here, we directly measured the chemical structures and bacterial and fungal communities of wheat (*Triticum aestivum* L.) and maize (*Zea mays* L.) residues after four-year decomposition in three Calcaric Fluvisols that varied in soil textures. Separation of the chemical structures among the six soil-straw combinations (two straw types × three soil textures) were generally coupled with trends in the communities of bacterial and fungal decomposers, but the nature of their coupling differed. In the sand soil, soil texture was the central feature that shaped bacterial and fungal communities for both straw types, driving in turn the convergence of chemical structures of both decomposing straws. In contrast, in the sandy loam and silty clay soils, straw type was the primary regulator of the colonizing bacterial and fungal communities, which resulted in the divergence of chemical structures according to straw type.

1. Introduction

The temporal changes in litter chemistry during decomposition have received increasing attention, but to date they have showed no consistent direction. Wickings et al. (2012) classified chemical pathways of litter decay into three patterns: (1) The "chemical convergence pattern", by which initially divergent litter chemistries generally converged when 75–80% of the initial mass had been lost (Preston et al., 2009; Wang et al., 2012; Bonanomi et al., 2018); (2) The "the initial litter quality control pattern", suggesting that initial differences in litter chemistry persisted throughout the decomposition process (Baumann et al., 2009; Li et al., 2015); and (3) The "decomposer control pattern", by which the types of decomposer communities exerted dominant control on the chemical changes in the decomposing litters (Šnajdr et al., 2011; Wickings et al., 2011). Each chemical pathway would result in distinct chemical characteristics of persistent residues, which represent a major fraction of soil organic matter (SOM) (Kubartová et al., 2009) and contribute significantly to soil ecosystem functioning (Kögel-Knabner, 2002).

Litter decomposition is widely believed to be carried out by a consortium of microbes, and both the bacterial and fungal communities associated with decomposing litter undergo rapid successional changes so that different taxa dominate temporarily at different decomposition stages (Voříšková and Baldrian, 2013; Maarastawi et al., 2018). It is generally accepted that the dominance of r-strategists that utilize easily degradable compounds in early stages is eventually replaced by K-strategists, which degrade recalcitrant substrates, in later stages of decomposition (Fierer et al., 2007; Bastian et al., 2009). However, this general progression could potentially be altered by selective role of initial litter quality on their degrading microbes (Aneja et al., 2006; Baumann et al., 2009) or the distinct microbial taxa in different soils (Mula-Michel and Williams, 2013). In addition, assembly history—the competitive and facilitative interactions between early colonizers and new immigrants—governs the succession of decomposer community structure (Fukami et al., 2010). It is possible that small differences in early assembly history result in substantial differences in subsequent microbial composition, which would make microbial evolution unpredictable (Fukami et al., 2010). Therefore, further information is

* Corresponding authors.
E-mail addresses: bzhao@issas.ac.cn (B. Zhao), jbzhang@mail.issas.ac.cn (J. Zhang).

https://doi.org/10.1016/j.apsoil.2020.103664
Received 3 March 2020; Received in revised form 14 May 2020; Accepted 16 May 2020
Available online 28 May 2020
0929-1393/ © 2020 Elsevier B.V. All rights reserved.

needed to clarify changes in the direction of decomposer community. Are they random or instead directionally constrained by ecological strategies of microbes, soil condition, or litter type?

Bonanomi et al. (2019) and Baumann et al. (2009) showed that chemical changes observed during decomposition interacted with shifts in microbial community composition. The replacement of r- by K-strategists during litter degradation could drive the convergence of chemical structure of residues to a recalcitrant nature (Berg and McClaugherty, 2008). However, other studies demonstrated that the regulatory effects of decomposer communities on chemical changes during litter decomposition were strongly influenced by initial litter type so that the imprints of initial chemistry persisted throughout the decomposition (Wickings et al., 2012; Wallenstein et al., 2013). Yet in other studies, changes in litter chemistry driven by decomposer communities also exhibited strong responses to specific soil conditions (Aneja et al., 2006; Wickings et al., 2011). This discrepancy may arise because simplistic broad categorization of microbial populations underestimates the divergent roles of decomposers having specific physiological capabilities (Wickings et al., 2011), so that changes in environmental factors (e.g. litter type or soil condition) could result in functionally different decomposer communities which could then modulate the chemical structure of residues. The relative importance of environmental factors in altering decomposer communities remains unclear.

The North China Plain (NCP) is a major agricultural production area in China, and has representative soil of Calcaric Fluvisol (FAO, 1998) with its texture ranging from sand to clay (Xia et al., 2015). Winter wheat and summer maize are widely grown in the NCP. Previous publications have shown that decomposer community composition could be altered by soil texture, probably through changing soil nutrition, moisture, and temperature conditions (Wickings et al., 2012; Mula-Michel and Williams, 2013).

In this study, we aimed to elucidate the specific directions of chemical and microbial changes of straw residues and their potential relationships, as influenced by straw type and soil textures. We directly assessed the chemical structures and microbial community compositions of residues persisting in the advanced decomposition stage at the NCP. Specifically, we buried wheat and maize straws in three Calcaric Fluvisol soils differing for their textures (sand, sandy loam, and silty clay), incubated for four years, and then detailed the chemical structures of the straws using solid-state ^{13}C nuclear magnetic resonance (^{13}C NMR) spectroscopy and residue-inhabiting microbial community compositions using 16S rRNA and ITS gene sequencing. The straw residues following four-year decomposition can be regarded as stable materials persisting after extensive decomposition, as we previously found that the straw masses decreased by 80% during an initial 10 months decomposition under conditions similar to those of the present study but decreased negligibly from 10 to 20 months (Li et al., 2020). We hypothesized that the chemical change of residues during degradation is depended on the dominant driver (straw type or soil textures) structuring decomposer communities.

2. Materials and methods

2.1. Study site and litterbag experiment

A long-term field experiment located in Pandian, Fengqiu Country, Henan province, China (114° 34′ E, 35° 01′ N) was initiated in 1992 to investigate the effects of soil texture on crop performance. The most common soil in this area is classified as a Calcaric Fluvisol (FAO, 1998). Three Calcaric Fluvisol soils differing from one another by having textures of sand, sandy loam, and silty clay were collected in 1992 from the villages of Huangling (114° 42′ E, 34° 58′ N), Pandian (114° 34′ E, 35° 01′ N), and Huangde (114° 25′ E, 35° 11′ N), respectively. Soil samples were collected at a depth of 0 to 60 cm from the three sites, and for each site, the surface layer (0 to 20 cm), center layer (20 to 40 cm), and bottom layer (40 to 60 cm) were collected separately. Then these soil samples were transferred to the study site in Pandian for placement into the experimental plots according to their original layer sequence. There were three replicated plots for each soil texture, giving a total of nine plots. Each plot (1.5 m wide × 2 m long × 0.6 m deep) was separated by cement banks that were 60 cm deep and extended 10 cm above the soil surface. The three sampling sites are about 50 km from each other, and therefore they shared the same climate, annual cropping system of winter wheat (October to May) and summer maize (June to September), and management strategies for > 50 years. From 1992 to 2012, annual crops with wheat and maize were cultivated under the same management regimes across all plots at the study site.

A litterbag experiment was initiated on December 4, 2012 in the nine plots. Some basic soil properties before the initiation are listed in Table S1. The wheat and maize straws were collected at harvest in June and October in 2012, respectively, from a nearby field, which has been under well-fertilized and crop management strategies common to the region. About 20 kg fresh wheat and 120 kg fresh maize straw were taken from five random quadrats (2 m × 2 m) in this field (about 3000 m^2). The straws were then cut into < 2 cm pieces, followed by air-drying in the laboratory, and incubated in litterbags (10 cm wide × 12.5 cm long) that were made of double-layer nylon mesh with mesh size of 0.074 mm. Each litterbag contained 15 g of air-dried (20–30 °C for 20 days) straw, which was equivalent to 13.67 g and 13.31 g of oven-dried (50 °C for 48 h) wheat straw and maize straw, respectively. The wheat straw contained: 450.1 ± 3.52 g C kg^{-1}; 8.41 ± 0.14 g N kg^{-1}; 0.58 ± 0.02 g P kg^{-1}; and 29.49 ± 0.94 g K kg^{-1}. The maize straw contained: 469.1 ± 2.47 g C kg^{-1}; 8.61 ± 0.17 g N kg^{-1}; 0.96 ± 0.03 g P kg^{-1}; and 11.93 ± 0.51 g K kg^{-1}. Carbon and N contents of the straw residues were determined using a Flash EA-Delta V (Flash-2000 Delta V Advantage, Thermo-Fisher, Germany). Straw P and K contents were digested by H_2SO_4 and H_2O_2 and then measured by molybdenum-blue method (Olsen et al., 1954) and flame photometer (FP640, Huayan, Shanghai, China), respectively. In the NCP, crop straws are usually returned back to the field on harvest, followed by mixing with the topsoil (0–15 cm) mechanically. To mimic the field condition, the litterbags were inserted vertically at 15 cm depth in each plot and were covered with a 5-cm layer of soil on the surface. Three litterbags of each straw type have been buried in each plot, resulting in a total 54 of litterbags (three soil textures × three replicates × two residue types × three replicates).

After four-year incubation, one wheat litterbag and one maize litterbag were sampled randomly from each of the three plots of each soil on December 4, 2016, resulting in a total of 18 litterbags (two residue types × three replicates × three soil textures). Adhered soil was gently removed from the bags and each residual straw sample was weighed with its mass recorded and then divided into two parts after thorough mixing. One part was oven-dried (50 °C for 48 h) for determining moisture content and adjustment of the mass of total residual sample, followed by grinding to pass through a 0.15 mm sieve for elemental and chemical structural analyses. The other part was stored at ambient field-moisture at −80 °C for DNA extraction.

The percentages of straw biomass, C, and N lost from the litterbag after four years were modeled using the equation: Biomass, C, or N loss (%) = $(M_0 - M_t)/M_0 \times 100$, where M_0 is the initial mass of biomass, C, or N of the straws, and M_t is the mass of biomass, C, or N of the straws remaining after four-year incubation.

2.2. Nuclear magnetic resonance spectroscopy

The chemical compositions of original and residual straws were assessed using advanced solid-state ^{13}C NMR spectroscopy. All the ^{13}C NMR experiments were carried out on a Bruker Avance 400 (Billerica, USA) spectrometer operating at a resonance frequency of 100 MHz for ^{13}C. Samples were packed into 4-mm sample rotors and run in a double-

resonance probe head. We combined samples from the three field replicates of each residue in each soil into one composite. The ^{13}C multiple cross-polarization magic-angle spinning (multiCP MAS) NMR spectra were recorded at a spinning speed of 14 kHz, with recycle delay of 0.35 s, and 90° ^{13}C pulse-length of 4 μs. All the obtained spectra have good signal-to-noise ratios, with minor (< 3%) spinning sidebands and limited overlap with center bands. To differentiate non-protonated C and mobile C from total C signal, ^{13}C multiCP MAS with dipolar dephasing was performed under the same conditions as for ^{13}C multiCP MAS but combined with a dipolar dephasing time of 68 μs (Cao et al., 2011).

The ^{13}C multiCP MAS spectra were segmented into eight chemical shift regions assigned to the following C functional groups (Mao and Schmidt-Rohr, 2004): alkyl C (0–44 ppm), methoxy/N-alkyl C (OCH_3/NCH) (44–64 ppm), O-alkyl C (64–93 ppm), anomeric C (93–113 ppm), aromatic C (113–142 ppm), aromatic C—O (142–162 ppm), carboxyl/amide C (162–188 ppm), and ketone/aldehyde C (C═O) (188–220 ppm).

The multiCP spectra with dipolar dephasing can further quantify non-protonated C and mobile C signals, which specifically permits separating the rotating CCH_3 and long-chained CH/CH_2 from alkyl C, OCH_3 and NCH from OCH_3/NCH, non-protonated O-alkyl C (OC_q) and protonated O-alkyl C (OCH) from O-alkyl C, and the non-protonated aromatic C (aromatic C—C) and protonated aromatic C (aromatic C—H) from aromatic C. The percentages of different functional groups were obtained by integrating and normalizing the spectral areas to the total signal intensity (0–220 ppm) for each spectrum.

2.3. DNA extraction, 16S rRNA and ITS gene amplification and sequencing, and bioinformatics analysis

Genomic DNA was extracted from 0.2 g decaying residue using the Fast DNA Spin Kit (MP Biomedicals, Santa Ana, CA, USA), following the manufacturer's instructions. DNA quantity and quality were assessed using a NanoDrop 2000 spectrophotometer (NanoDrop Technologies, Wilmington, DE, USA). DNA was stored at −80 °C until further analysis.

The V4–V5 region of bacterial 16S rRNA gene and the ITS1 region of fungal internal transcribed spacer (ITS) were amplified using primer pairs 515F/907R (5′-GTGCCAGCMGCCGCGGTAA-3′/5′-CCGTCAATTCMTTTRAGTTT-3′) and ITS5F/ITS1R (5′-GGAAGTAAAAGTCGTAACAAGG-3′/5′-GCTGCGTTCTTCATCGATGC-3′), respectively. The polymerase chain reaction (PCR) amplification was performed using a 25 μl reaction mixture, containing 2 μl (2.5 mM) of dNTPs, 0.25 μl of Q5 high-fidelity DNA polymerase (5 U/μl), 1 μl (10 μM) of each forward and reverse primer, 5 μl of Q5 reaction buffer (5×), 2 μl of DNA template, 5 μl of Q5 high-fidelity GC buffer (5×), and 8.75 μl of ddH_2O. The thermal cycling for bacteria consisted of initial denaturation at 98 °C for 5 min, followed by 24 cycles consisting of 98 °C for 30 s, 52 °C for 30 s, and 72 °C for 1 min, with a final extension at 72 °C for 5 min. The thermal cycling for fungi consisted of initial denaturation at 98 °C for 5 min, followed by 28 cycles consisting of 98 °C for 30 s, 52 °C for 30 s, and 72 °C for 1 min, with a final extension at 72 °C for 5 min.

The PCR products were purified with Agencourt AMPure Beads (Beckman Coulter, Indianapolis, IN) and quantified using the PicoGreen dsDNA Assay Kit (Invitrogen, Carlsbad, CA, USA). The purified PCR products were pooled in equal amounts and sequenced using the Illlumina MiSeq platform. Raw Sequence data have been submitted to the NCBI Sequence Read Archive database under accession numbers SUB6360544 and SUB6366319.

The Quantitative Insights into Microbial Ecology (QIIME, USA) pipeline was used to process the sequence data (Caporaso et al., 2010). In brief, sequences with an average Phred scores of < 20, a length of < 150 bp, exact matches to the barcodes and primers, and containing mononucleotide repeats of > 8 bp as well as ambiguous bases were filtered for further analysis (Gill et al., 2006; Chen and Jiang, 2014). After paired-end reads assembly and chimera detection, the remaining high-quality sequences were clustered into operational taxonomic units (OTUs) based on 97% identity threshold using UCLUST (Edgar, 2010). The most abundance sequence for each OTU was selected as the representative sequence. Bacterial 16S rRNA and fungal ITS OTU representative sequences were aligned against the Greengenes database (v. 13.8) (DeSantis et al., 2006) and the UNITE database (Kõljalg et al., 2013), respectively. Non-bacterial and non-fungal sequences and rare taxa (containing < 0.001% of total sequences) were discarded and the remaining sequences of all the samples were then rarefied to the same sequencing depth (16919 for 16S rRNA and 26195 for ITS) for downstream analysis. Principal coordinate analysis (PCoA) of the weighted UniFrac distance was measured to assess the bacterial and fungal community dissimilarities among samples.

2.4. Statistical analyses

Two-way analyses of variance (ANOVA) followed by a least significant difference multiple-comparison test was conducted to identify significant effects of soil texture and straw type on losses of straw biomass, C, and N as well as on the bacterial and fungal taxa. The normality and homogeneity of all variables were tested using the Kolmogorov-Smirnov test and the Levene statistic, respectively.

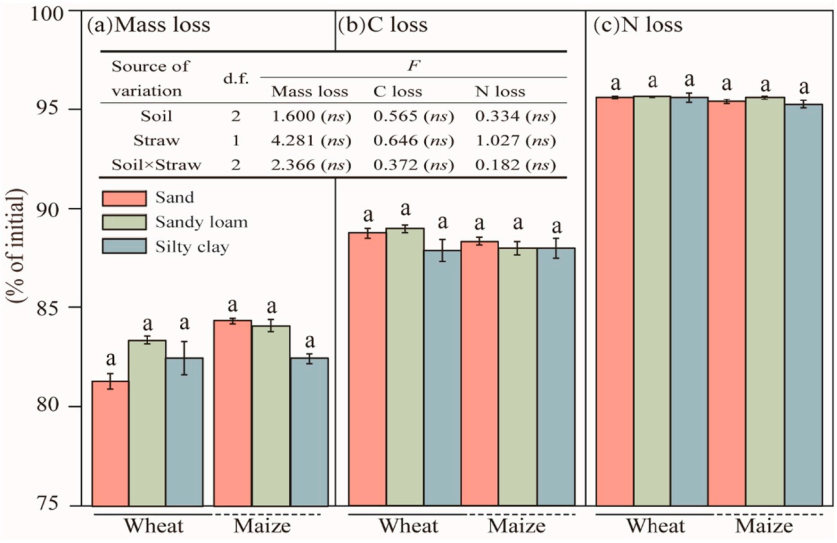

Fig. 1. Mass losses of biomass, carbon (C), and nitrogen (N) in the residual straws of wheat and maize after four-year decomposition in three Calcaric Fluvisol soils differing by texture (sand, sandy loam, and silty clay). Vertical bars denote the standard errors of the means. Same lowercase letters above the bars indicate no significant differences ($P > 0.05$) for that specific parameter. "*ns*" indicates no significant differences ($P > 0.05$) for that specific parameter.

Table 1
Percentages of total spectral area (%) assigned to different functional groups resolved by ^{13}C multiCP magic angle spinning (MAS) nuclear magnetic resonance and dipolar dephased multiCP MAS before ("original") and after four-year decomposition of two straw types in three Calcaric Fluvisol soils differing by texture (sand, sandy loam, and silty clay).

Straw	Soil	220–188 ppm	188–162 ppm	162–142 ppm	142–113 ppm		113–93 ppm	93–64 ppm		64–44 ppm			44–0 ppm		
		Ketone/aldehyde C	Carboxyl/amide C	Aromatic C−O	Aromatic C		Anomeric C	O-alkyl C		OCH_3/NCH			Alkyl C		
					Total	Arom. C−C	Arom. C−H		Total	OCq	OCH	Total	OCH_3	NCH	Total	CCH_3	CH/CH_2
Wheat	Original	0.89	3.20	2.62	5.50	0.97	4.53	13.93	51.06	1.14	49.91	12.25	1.60	10.64	10.56	2.58	7.98
	Sand	1.76	8.41	5.50	13.09	6.02	7.07	9.96	26.09	2.24	23.85	16.44	4.55	11.89	18.76	3.92	14.84
	Sandy loam	1.41	8.01	5.11	11.56	5.92	5.64	9.94	26.98	2.29	24.70	16.05	4.56	11.49	20.94	4.88	16.05
	Silty clay	1.18	8.12	5.22	12.6	5.67	6.94	10.01	27.56	2.38	25.18	15.98	4.38	11.60	19.34	4.28	15.05
Maize	Original	0.62	4.19	3.17	6.26	2.20	4.07	12.24	48.44	2.24	46.19	12.94	2.15	10.78	12.14	3.16	8.98
	Sand	2.03	9.20	5.69	13.88	6.12	7.75	9.46	25.92	2.70	23.22	16.22	4.95	11.27	17.61	3.95	13.66
	Sandy loam	1.28	7.60	5.78	13.52	6.05	7.47	10.77	30.29	2.47	27.81	15.85	4.39	11.46	14.91	3.69	11.22
	Silty clay	2.28	8.50	5.75	13.01	5.51	7.51	10.20	29.27	1.89	27.38	15.28	3.88	11.40	15.70	3.59	12.12

Significant differences were defined as $P < 0.05$ unless the *P*-values are reported.

The principal component analysis (PCA) was employed to exhibit chemical differences among treatments based on NMR data by using R statistical software v3.3.3 with the vegan package (Dixon, 2003). Permutational multivariate analysis of variance (PERMANOVA) was conducted to determine the significant differences in microbial communities among treatments using the "adonis2" function in the vegan package, and the differential OTUs among treatments were distinguished by using the edgeR package. Similarity percentage analysis (SIMPER) was also conducted to reveal dissimilarities in microbial communities among treatments and to identify the key OTUs contributing to the observed differences (Clarke, 1993). The overall relationships between chemical composition and bacterial and fungal community composition were compared using the Mantel test (999 permutations) in the vegan package.

To explore the co-occurrence patterns among chemical structure and microbial communities in decaying residue, we calculated all possible pair-wise Spearman's rank correlations between residual C-functional groups and bacterial and fungal OTUs using the psych package. The obtained *P*-values were adjusted for multiple comparisons using the false discovery rate at 0.05 level. To reduce network complexity, we only considered the OTUs that exhibited significant difference between treatments and also contained > 0.1% of total sequences assigned to bacteria and 0.01% of sequences assigned to fungi. The selected 90 bacterial OTUs, 120 fungal OTUs, and five C-functional groups with either strong positive (Spearman's correlation coefficient > 0.6, $P < 0.05$) or strong negative (Spearman's correlation coefficient < -0.6, $P < 0.05$) relationships were used for constructing a network in Cytoscape v.3.4.0. We calculated the network topological features using the NetworkAnalyzer tool and the modularity using MCODE plugin in Cytoscape.

3. Results

3.1. Weight losses of straw biomass, C, and N

Averaged across straw types and soil textures, 83.1%, 88.4%, and 95.6% of the original masses of straw biomass, C, and N respectively, were lost after four-year decomposition (Fig. 1). The ANOVA results further revealed that their losses were not significantly affected by straw type or soil texture ($P > 0.05$, Fig. 1).

3.2. Chemical structure

The chemical structures of the initial two straws were dominated by OCH, accounting for 49.9% of the total C in wheat and 46.2% in maize straw (Table 1; Fig. S1). The initial maize straw exhibited higher CH/CH_2 abundance than did the initial wheat straw. After four-year decomposition, there were substantial decreases in the abundances of OCH (by 25.3% in wheat and 20.1% in maize) and anomeric C (by 3.96% in wheat and 2.10% in maize) and increases in the abundances of other C functional groups across soil textures, particularly CH/CH_2 (by 7.34% in wheat and 3.36% in maize) and carboxyl/amide C (by 4.90% in wheat and 4.24% in maize) (Table 1).

The PCA performed on the relative abundances of functional groups in the residues following decomposition showed that the chemical structures among the six soil-straw combinations (two straw types × three soil textures) could be separated into three groups (Fig. 2). The first group contained both wheat and maize residues in the sand soil, which had the lowest OCH and highest carboxyl/amide C abundances; the second group contained only wheat residues in the sandy loam and silty clay soils, which exhibited the lowest aromatic C−H and highest CH/CH_2 abundances; and the third group contained only maize residues in the sandy loam and silty clay soils, which showed the lowest CH/CH_2 and highest OCH abundances.

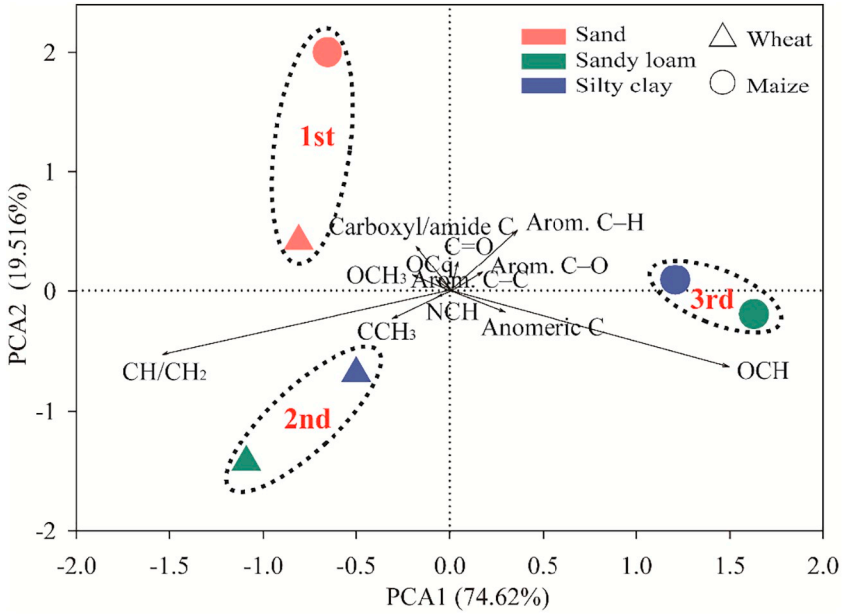

Fig. 2. Combined ordination plot of principal component analysis (PCA) performed on the relative abundances of 12 C functional groups for the residual straws of wheat and maize after four years decomposition in three Calcaric Fluvisol soils differing by texture (sand, sandy loam, and silty clay).

3.3. Microbial community composition of the residues

Major bacterial phyla were present in all residual straws, of which Proteobacteria accounted for 36.6 ± 0.13% of the total sequences, followed by the Actinobacteria (21.8 ± 0.24%), Chloroflexi (13.1 ± 0.15%), and Acidobacteria (9.08 ± 0.08%) (Fig. 3a). Within the Proteobacteria, Alphaproteobacteria (20.0 ± 0.13%) showed the highest relative abundance. Both wheat and maize straw in the sand soil had the lowest Actinobacteria abundance, while the wheat straw in the sandy loam and silty clay soils had the lowest Acidobacteria abundance ($P < 0.05$).

Ascomycota comprised 86.6 ± 0.59% of all fungal sequences in the six soil-straw combinations (Fig. 3b). Regarding the major fungal genera, both wheat and maize straws in the sand soil were dominated by unclassified Coniochaetales, comprising 73.2 ± 1.63% of the total sequence, but this genus was barely detected in the other treatments (Fig. 3b). The relative abundances of the fungal genera were more similar in the sandy loam and silty clay soils, with the predominant fungal genera in the wheat straws being Pseudogymnoascus (37.5 ± 2.01%) and Acremonium (17.1 ± 2.21%), and in the maize straws being Pseudogymnoascus (17.9 ± 1.05%) and unclassified Lasiosphaeriaceae (14.5 ± 1.42%) (Fig. 3b).

The PCoA with weighted distance results both for bacterial and fungal communities were clearly separated among the six soil-straw treatments into the same three groups as for the PCA pattern of the NMR results (Figs. 2 and 4). Namely, the first group contained both wheat and maize residues in the sand soil, the second contained only wheat residues in the sandy loam and silty clay soils, and the third contained only maize residues in the sandy loam and silty clay soils (Fig. 4). The results of PERMANOVA further confirmed the significant differences among these three groups ($P < 0.01$, Table 2).

The edgeR and SIMPER analyses were performed to identify the key OTUs contributing to the differences of bacterial or fungal communities among the three soil-straw combination groups (Fig. 5; Tables S2 and S3). Specifically, the species that most contributed to the divergences of bacterial communities among the three groups were the dominant *Jiangella* sp. and unclassified members of Cytophagaceae, Chloroflexi, Anaerolineae, and Bacillales in the first group, the enriched members of Solirubrobacterales, Cytophagaceae, Anaerolineae, Pirellulaceae, and Acidimicrobiales in the second group, and the abundant *Solirubrobacter* sp., *Microbacterium* sp., and unclassified members of Sinobacteraceae, Acidobacteria subgroup 6, Solirubrobacterales, Acidimicrobiales, and Cytophagaceae in the third group (Fig. 5a; Table S2).

The divergences of fungal communities among the three groups were mainly attributed to the overwhelming dominance of specialized *Coniochaetales* sp. in the sand soil, whereas more diverse fungal species distributed in the other two groups, including the abundant *Pseudogymnoascus roseus* sp., *Acremonium psammosporum* sp., and *Coniochaeta* sp. in the wheat residues in the sandy loam and silty clay soils, and the enriched *Lecythophora* sp., *Agaricales* sp., *Microascales* sp., and *Pyrenochaetopsis* sp. in the maize residues in the same two soils (Fig. 5b; Table S3).

3.4. Relationships between chemical structure and microbial community composition

Overall, there were significant ($P < 0.001$) and positive interactions between the chemical structures of the residual straws and their associated bacterial and fungal communities (Table S4). To further characterize their relationships, network analysis associated bacterial and fungal taxa with C functional groups (Fig. 6). The network comprising of 216 nodes and 3879 edges was partitioned into seven modules. The highly interconnected relationships among C groups and the microbial taxa in the first three modules suggested that they represent the functional core of the network. Specifically, module I was composed of OCH, CH/CH_2, and 41 bacterial and 17 fungal OTUs. Module II was dominated by aromatic C—H and 33 bacterial and 16 fungal OTUs. Module III included carboxyl/amide C and 10 bacterial and 6 fungal OTUs.

The abundance of OCH was negatively connected with *Jiangella* sp., unclassified Chloroflexi and *Coniochaetales* sp. and positively connected with *Solirubrobacter* sp., *Microbacterium* sp. and unclassified members of Acidobacteria subgroup 6 and Acidimicrobiales (Fig. 6). The CH/CH_2 showed negative associations with unclassified Sinobacteraceae, unclassified Solirubrobacterales, *Microbacterium* sp., *Lecythophora* sp., *Microascales* sp., and *Pyrenochaetopsis* sp., and positive associations with *Pseudogymnoascus roseus* sp.. The aromatic C—H abundance was negatively associated with *Pseudogymnoascus roseus* sp. and *Acremonium psammosporum* sp.. In addition, the carboxyl/amide C abundance showed a positive association with unclassified Bacillales.

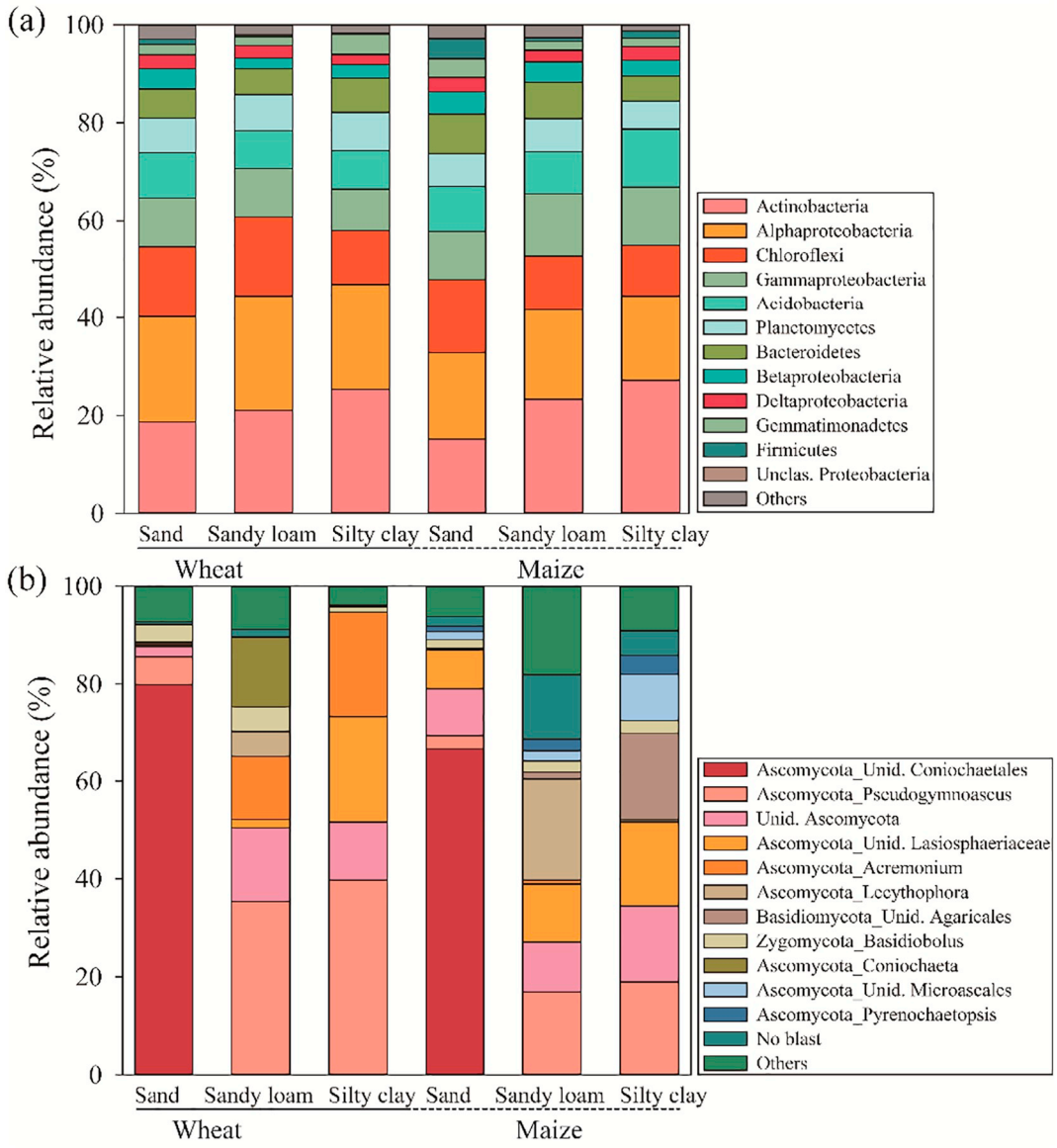

Fig. 3. Relative abundances of the major bacterial phyla and dominant classes of Proteobacteria (a) and the major fungal genera (b) in the residual straws of wheat and maize after four years decomposition in three Calcaric Fluvisol soils differing by texture (sand, sandy loam, and silty clay).

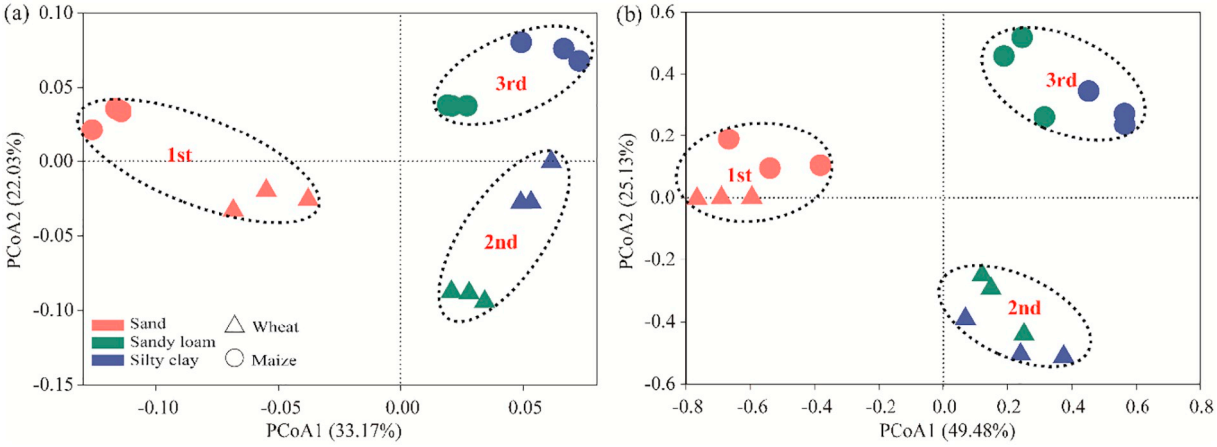

Fig. 4. Principal coordinate analysis (PCoA) plots depicting the weighted UniFrac distance of bacterial communities (a) and fungal communities (b) in the residual straws of wheat and maize after four years decomposition in three Calcaric Fluvisol soils differing by texture (sand, sandy loam, and silty clay).

Table 2
Differences of bacterial and fungal composition between residual straws after four-year decomposition based on PERMANOVA analyses.

Group A	Group B	Bacterial composition		Fungal composition	
		F	*P*	*F*	*P*
First group	Second group	8.18	0.005**	30.88	0.002**
First group	Third group	9.94	0.003**	21.89	0.004**
Second group	Third group	6.51	0.001**	7.3	0.006**

** indicates significant at $P < 0.01$.

4. Discussion

4.1. Deviations of chemical structure in straw residues after four-year decomposition

Generally, the chemical changes in the decomposing straw residues were in accordance with the decay trajectory elaborated by many studies (Preston et al., 2009; Wang et al., 2012; Bonanomi et al., 2018), the loss of easily decomposable compounds, characterized by ^{13}C NMR as O-alkyl and anomeric C, causing relative enrichment of more recalcitrant compounds such as aliphatic and aromatic materials. However, distinct differences in chemical composition, which were quantified by advanced solid-state NMR techniques, still existed between residues at four years by which time 83% of the original biomass had been lost (Table 1; Fig. 1).

The convergence of initially distinct chemical compositions of wheat and maize straws after four-year decomposition in the sand soil is consistent with some previous studies, which found that initially divergent litter chemistries generally converged when 75–80% of the initial mass had been lost (Preston et al., 2009; Wang et al., 2012; Bonanomi et al., 2018). In the sandy loam and silty clay soils, however, the changes in chemical structure during decomposition deviated between the two straw types. Specifically, the initial wheat straw in both soils exhibited higher OCH but lower CH/CH_2 abundances than the maize straw, whereas, the wheat straw showed lower OCH but higher CH/CH_2 abundances than the maize straw after four-year decomposition (Table 1). This kind of divergence according to straw type in these two finer-textured soils seems partially contradictory to the reports showing that the imprints of initial chemistry persisted throughout the decomposition (Wickings et al., 2012; Wallenstein et al., 2013; Parsons et al., 2014). This results suggest that, during four-year decomposition, specific microbial communities with distinct C-related decomposition strategies might have developed that led to the differentiation of three soil-straw combination groups of chemical structure.

4.2. Deviations of microbial composition in residues after four-year decomposition

After four-year decomposition, the dominant abundance of Alphaproteobacteria and Actinobacteria, which belonged to bacteria with K-strategists (Senechkin et al., 2010; Di Lonardo et al., 2017), was consistent with their marked superiority at the advanced stages of decomposition reported in other studies (Dilly et al., 2004; Šnajdr et al., 2011; Mula-Michel and Williams, 2013; Moitinho et al., 2018). However, the overwhelming dominance of Ascomycota, which were generally known as fungal cellulose decomposers, was in contrast to the reported replacement of Ascomycota by recalcitrant compound decomposer-Basidiomycota during litter degradation (Voříšková and Baldrian, 2013; Purahong et al., 2016). This may relate to the dominance of OCH group, which is considered as easily degradable (Kögel-Knabner, 2002).

The bacterial and fungal communities among the six soil-straw combinations were clustered into the same three straw-soil combination groups as for chemical structure. The bacterial community of the first group exhibited the most abundant *Jiangella* sp., when compared with the second or third groups. Given that *Jiangella* sp. has thus far been described as aerobic filamentous bacteria (Estrada-Medina et al., 2016), its abundance may be related to the high degree of aeration that would prevail in the sand soil that defined the first group. Simultaneously, the fungal community of the first group was especially dominated by opportunistic *Coniochaetales* sp. (73.2 ± 1.63% of the total sequence), indicating a competitive exclusion of other taxa, while a more diverse array of fungal species was heterogeneously distributed within the second and third groups. One speculative explanation for this observation centers on soil nutrient availability, which Siciliano et al. (2014) associated with fungal richness and diversity. Relative to the sandy loam and silty clay soils, the sand soil was deficient in various nutrients (Table S1), which may induce competition among species, resulting in the competitive exclusion by the opportunistic *Coniochaetales* sp. of other taxa (Hardin, 1960). On the contrary, the sandy loam or silty clay soils had higher nutrients contents (Table S1), which may alleviate the competition among species, resulting in coexistence of diverse fungal species.

4.3. Linkages between chemical structure and microbial composition

The chemical structure of decaying residues was positively associated with both bacterial and fungal community composition, suggesting that chemical change was coupled with microbial variation. This was consistent with the findings of Liu et al. (2016) and Bonanomi et al. (2019) who described the close relationship between the temporal dynamics of litter chemistry and decomposer composition over 7-month and 180-day periods, respectively.

More specifically, the most significant taxa in the wheat and maize residues of the first group, including *Jiangella* sp., unclassified Chloroflexi, and *Coniochaetales* sp. abundances, were negatively associated with OCH abundance. Among them, the *Jiangella* sp. could potentially degrade polysaccharide (Lladó et al., 2016), the Chloroflexi species were previously identified as cellobiose-degrading bacteria (Baker et al., 2015), and *Coniochaetales* sp. was identified as a fast growing opportunistic saprotroph (Weber et al., 2015) that may participate in the utilization of easily degradable fraction. Consequently, the enrichment of these microbial species may result in the decrease of OCH abundance in the first group. Meanwhile, the higher carboxyl/amide C abundance observed in the first group may be related to their abundant unclassified member of Bacillales, which was found to be involved in the oxygenation of lignin polymers (Martins et al., 2013) and may contribute to the production of carboxylic acid (Hilscher and Knicker, 2011). Alternatively, the greater loss of OCH in this first group compared to the other two groups might lead to selective enrichment of compounds such as carboxyl that are associated with advanced states of decomposition (Zech et al., 1997). The specific OCH-related metabolism in the sand soil might reflect the dominance of the soil texture effect over the straw type effect.

In the second group, the wheat residues were significantly enriched with *Pseudogymnoascus roseus* sp., which exhibited negative correlation with aromatic C—H and positive correlation with CH/CH_2 abundances. Batista-García et al. (2017) reported that Pseudogymnoascus displayed high ligninolytic enzymes activities. We postulate that the *Pseudogymnoascus roseus* sp. may be involved in the degradation of aromatic structure, followed by the formation of aliphatic groups (Geng and Li, 2002). Meanwhile, the observed negative association between the *Acremonium psammosporum* sp. and the aromatic C—H abundance may relate to the lignocellulolytic capability of Acremonium species (Rime et al., 2016).

In the third group, the highly enriched species in the maize residues including *Solirubrobacter* sp., *Microbacterium* sp. and unclassified members of Acidobacteria subgroup 6 and Acidimicrobiales, were positively associated with OCH abundance. Among them, the *Solirubrobacter* species were reported to be involved in complex

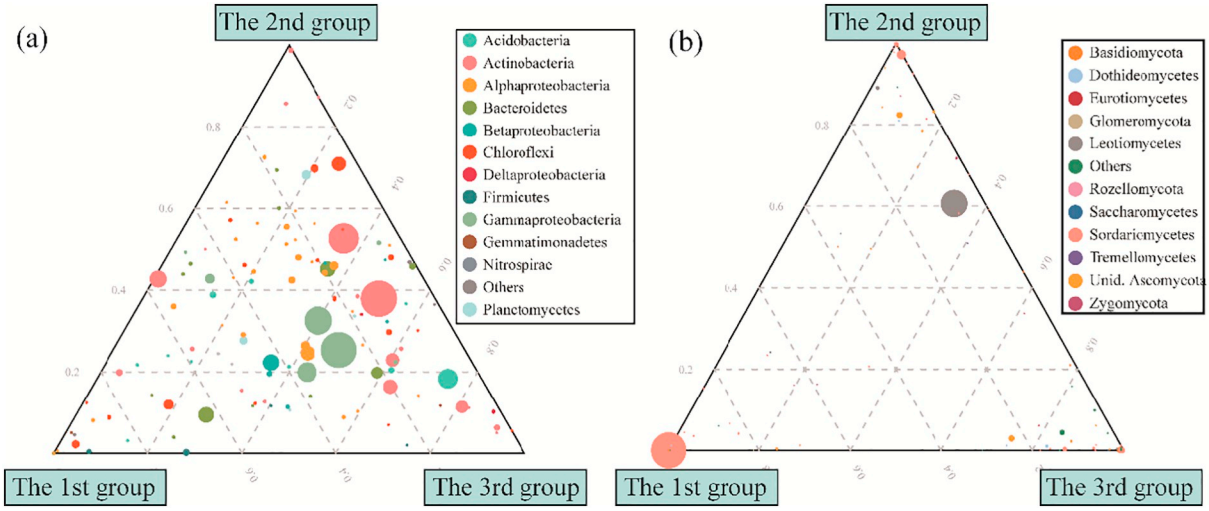

Fig. 5. Ternary plots indicating the distribution of bacterial (a) and fungal (b) OTUs from three groups. Circle size represents the average abundance of the OTU, and location represents their proportional abundances in the three groups. Circle color represents the corresponding OTUs assigned to major phyla or classes.

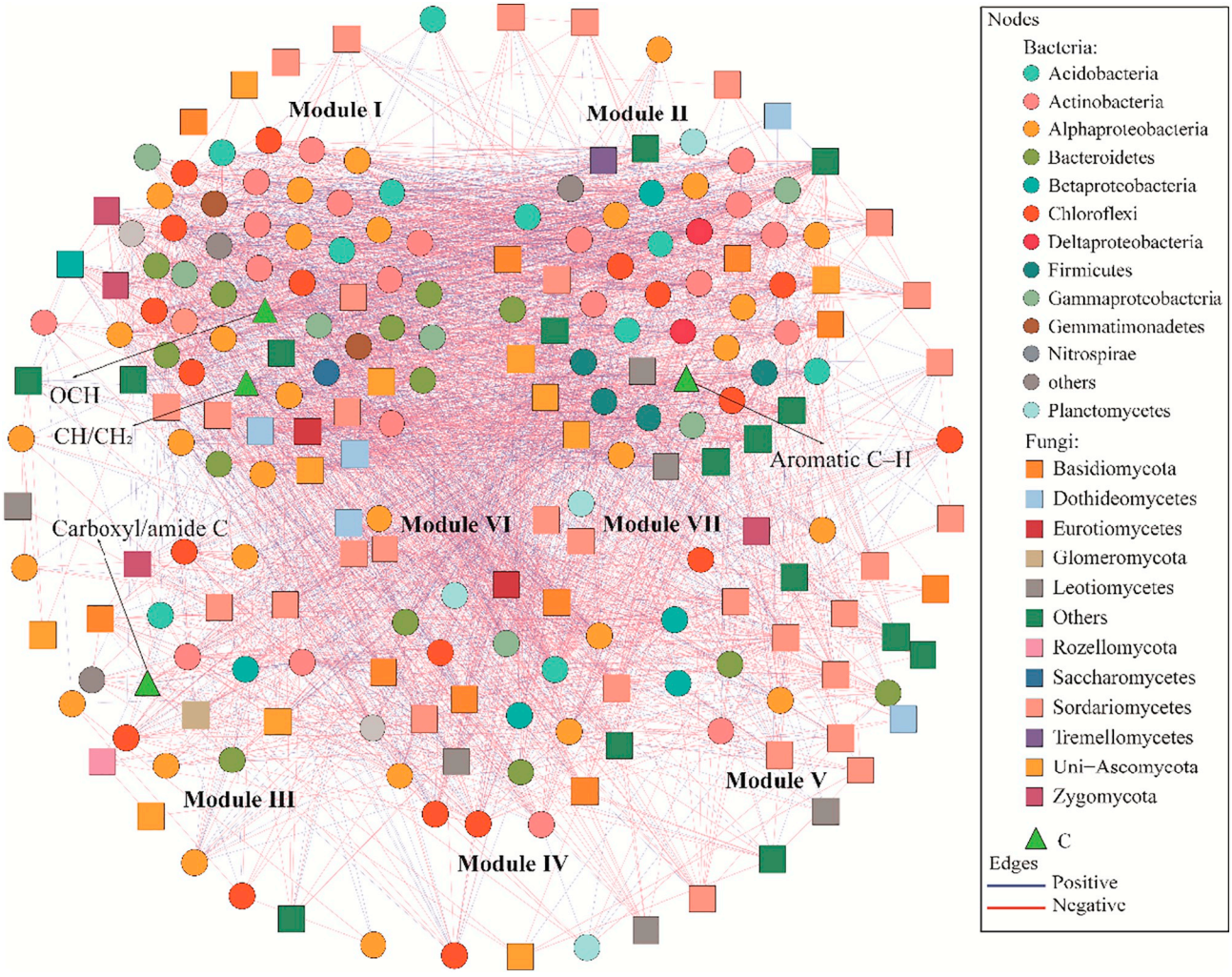

Fig. 6. Network analysis revealing the associations among bacterial and fungal taxa and C functional groups. Blue and red lines represent strong positive (Spearman's correlation coefficient > 0.6, $P < 0.05$) and strong negative (Spearman's correlation coefficient < -0.6, $P < 0.05$) relationships, respectively. Colored nodes signify corresponding OTUs assigned to major phyla and classes. C functional groups are indicated with triangles. (For interpretation of the references to color in this figure legend, the reader is referred to the web version of this article.)

glycoside degradation (Jacquiod et al., 2013). Members of *Microbacterium* have significant starch hydrolysis activities (Lee et al., 2014) and β-glucosidase catalytic activities (Park et al., 2008). Acidimicrobiales are known to be involved in plant degradation by secreting glycoside hydrolases and carbohydrate esterases (Zhang et al., 2015). Therefore, all these species could break down complex polymers and consequently form free sugars, which may result in the accumulation of OCH groups. Meanwhile, the dominant species, including Sinobacteraceae, Solirubrobacterales, *Microbacterium* sp., and *Microascales* sp., showed negative associations with CH/CH_2 abundance (Fig. 6), probably because of their capability to metabolize aliphatic hydrocarbon compounds (Manickam et al., 2006; Gutierrez et al., 2013; Abbasian et al., 2016; Blasi et al., 2016; Galitskaya et al., 2016).

Li et al. (2020) reported for earlier samplings of these same straw residues that the readily decomposable O-alkyl and anomeric C components of the wheat straw were effectively broke down by sugar fungi, while in the maize straw the refractory lignin components were preferentially degraded by the abundant ligninolytic fungi. In the present study, the relationships between the enriched microbial species and aromatic C−H degradation in the wheat residues in the sandy loam and silty clay soils (Fig. 6) suggested that once the readily decomposable components in wheat straw were adequately broken down in the earlier stage, then the lignin may become the major component to be degraded at the advanced decomposition stage. Likewise, in the maize residues in the sandy loam and silty clay soils, the relationship between the dominant microbial species and glycoside and CH/CH_2 degradation (Fig. 6) suggested a transition of degradation from intense lignin degradation to glycoside and CH/CH_2 degradation due to widespread consumption of lignin compounds already in the earlier stages of decomposition. However, the measurements conducted in this study do not enable a clear reason for the hypothesized faster degradation of lignin in the wheat residues than in maize residues.

The drive effect of decomposer community on the chemical structure of wheat and maize straws in the sandy loam and silty clay soils was regulated by straw type, in accordance with Wickings et al. (2012), who suggested that the divergent chemistry of corn and grass litters throughout a 730-day decay period was driven by differences in decomposer communities, which was impacted by initial litter chemistry. Liu et al. (2016) also reported coupled divergence of chemical and microbial composition by litter type in a finer-textured (silty loam) soil. Whereas in the sand soil, we found that both the chemical structures and the inhabiting microbial communities converged to common points across straw types after four years of decomposition, suggesting their primary constraint was soil conditions. Similar results were obtained by García-Palacios et al. (2016) showing the convergences of chemical structures and microbial communities after 11-month decomposition of leaf litter mixtures that were placed on five different forest floors. A possible explanation for this might be the fully aerobic conditions during leaf litter degradation, possibly resembling those of our sand soil. Our results implied that the previously observed convergences or divergences of chemical and microbial composition during decay might not be inconsistent, but they were determined by varying biotic and abiotic environments in which the decomposition occurred.

5. Conclusions

Our results emphasized a dominate role of residue-inhabiting microbial communities in shaping the chemical structure of straw residues. Yet both soil texture and straw type could regulate the bacterial and fungal communities harboured in the residue layer and thereby modulate the chemical structures. The relative importance of soil texture and straw type depended on the soil conditions during degradation. The chemically distinct compounds remaining after prolonged decomposition were considered as part of SOM, which underscores the potential usefulness of our results for assessing the quality and stability of litter-derived organic matter in field ecosystems.

Declaration of competing interest

The authors declare that they have no known competing financial interests or personal relationships that could have appeared to influence the work reported in this paper.

Acknowledgements

This work was financially supported by the National Key Research and Development Program of China (2016YFD0300802), National Natural Science Foundation of China (41977102), and the China Agriculture Research System (CARS-03).

Appendix A. Supplementary data

Supplementary data to this article can be found online at https://doi.org/10.1016/j.apsoil.2020.103664.

References

Abbasian, F., Palanisami, T., Megharaj, M., Naidu, R., Lockington, R., Ramadass, K., 2016. Microbial diversity and hydrocarbon degrading gene capacity of a crude oil field soil as determined by metagenomics analysis. Biotechnol. Prog. 32, 638–648.
Aneja, M.K., Sharma, S., Fleischmann, F., Stich, S., Heller, W., Bahnweg, G., Munch, J.C., Schloter, M., 2006. Microbial colonization of beech and spruce litter—influence of decomposition site and plant litter species on the diversity of microbial community. Microb. Ecol. 52, 127–135.
Baker, B.J., Lazar, C.S., Teske, A.P., Dick, G.J., 2015. Genomic resolution of linkages in carbon, nitrogen, and sulfur cycling among widespread estuary sediment bacteria. Microbiome 3, 14.
Bastian, F., Bouziri, L., Nicolardot, B., Ranjard, L., 2009. Impact of wheat straw decomposition on successional patterns of soil microbial community structure. Soil Biol. Biochem. 41, 262–275.
Batista-García, R.A., Sutton, T., Jackson, S.A., Tovar-Herrera, O.E., Balcázar-López, E., Sánchez-Carbente, M.D., Sánchez-Reyes, A., Dobson, A.D.W., Folch-Mallol, J.L., 2017. Characterization of lignocellulolytic activities from fungi isolated from the deep-sea sponge Stelletta normani. PLoS One 12, e0173750.
Baumann, K., Marschner, P., Smernik, R.J., Baldock, J.A., 2009. Residue chemistry and microbial community structure during decomposition of eucalypt, wheat and vetch residues. Soil Biol. Biochem. 41, 1966–1975.
Berg, B., McClaugherty, C., 2008. Plant Litter Decomposition, Humus Formation, Carbon Sequestration, second ed. Springer, Berlin, Heidelberg.
Blasi, B., Poyntner, C., Rudavsky, T., Prenafeta-Boldú, F.X., De Hoog, S., Tafer, H., Sterflinger, K., 2016. Pathogenic yet environmentally friendly? Black fungal candidates for bioremediation of pollutants. Geomicrobiol J. 33, 308–317.
Bonanomi, G., Incerti, G., Abd El-Gawad, A.M., Cesarano, G., Sarker, T.C., Saulino, L., Lanzotti, V., Saracino, A., Rego, F.C., Mazzoleni, S., 2018. Comparing chemistry and bioactivity of burned vs. decomposed plant litter: different pathways but same result? Ecology 99, 158–171.
Bonanomi, G., De Filippis, F., Cesarano, G., La Storia, A., Zotti, M., Mazzoleni, S., Incerti, G., 2019. Linking bacterial and eukaryotic microbiota to litter chemistry: combining next generation sequencing with ^{13}C CPMAS NMR spectroscopy. Soil Biol. Biochem. 129, 110–121.
Cao, X., Olk, D.C., Chappell, M., Cambardella, C.A., Miller, L.F., Mao, J., 2011. Solid-state NMR analysis of soil organic matter fractions from integrated physical-chemical extraction. Soil Sci. Soc. Am. J. 75, 1374–1384.
Caporaso, J.G., Kuczynski, J., Stombaugh, J., Bittinger, K., Bushman, F.D., Costello, E.K., Fierer, N., Peña, A.G., Goodrich, J.K., Gordon, J.I., Huttley, G.A., Kelley, S.T., Knights, D., Koenig, J.E., Ley, R.E., Lozupone, C.A., McDonald, D., Muegge, B.D., Pirrung, M., Reeder, J., Sevinsky, J.R., Tumbaugh, P.J., Walters, W.A., Widmann, J., Yatsunenko, T., Zaneveld, J., Knight, R., 2010. QIIME allows analysis of high-throughput community sequencing data. Nat. Methods 7, 335–336.
Chen, H., Jiang, W., 2014. Application of high-throughput sequencing in understanding human oral microbiome related with health and disease. Front. Microbiol. 5, 508.
Clarke, K.R., 1993. Non-parametric multivariate analyses of changes in community structure. Aust. J. E. 18, 117–143.
DeSantis, T.Z., Hugenholtz, P., Larsen, N., Rojas, M., Brodie, E.L., Keller, K., Huber, T., Dalevi, D., Hu, P., Andersen, G.L., 2006. Greengenes, a chimera-checked 16S rRNA gene database and workbench compatible with ARB. Appl. Environ. Microbiol. 72, 5069–5072.
Di Lonardo, D.P., De Boer, W., Gunnewiek, P.J.A.K., Hannula, S.E., Van der Wal, A., 2017. Priming of soil organic matter: chemical structure of added compounds is more important than the energy content. Soil Biol. Biochem. 108, 41–54.
Dilly, O., Bloem, J., Vos, A., Munch, J.C., 2004. Bacterial diversity in agricultural soils during litter decomposition. Appl. Environ. Microb. 70, 468–474.
Dixon, P., 2003. VEGAN, a package of R functions for community ecology. J. Veg. Sci. 14, 927–930.
Edgar, R.C., 2010. Search and clustering orders of magnitude faster than BLAST. Bioinformatics 26, 2460–2461.

Estrada-Medina, H., Canto-Canché, B.B., De los Santos-Briones, C., O'Connor-Sánchez, A., 2016. Yucatán in black and red: linking edaphic analysis and pyrosequencing-based assessment of bacterial and fungal community structures in the two main kinds of soil of Yucatán State. Microbiol. Res. 188, 23–33.
FAO, 1998. World Reference Base for Soil Resources. World Soil Resources. Report 84. FAO, Rome.
Fierer, N., Bradford, M.A., Jackson, R.B., 2007. Toward an ecological classification of soil bacteria. Ecology 88, 1354–1364.
Fukami, T., Dickie, I.A., Wilkie, J.P., Paulus, B.C., Park, D., Roberts, A., Buchanan, P.K., Allen, R.B., 2010. Assembly history dictates ecosystem functioning: evidence from wood decomposer communities. Ecol. Lett. 13, 675–684.
Galitskaya, P., Biktasheva, L., Selivanovskaya, S., 2016. Bacterial community composition changes in the process of oily waste remediation using compost. Int. Multi. Sci. Geoco. 3, 193–200.
García-Palacios, P., Shaw, E.A., Wall, D.H., Hättenschwiler, S., 2016. Temporal dynamics of biotic and abiotic drivers of litter decomposition. Ecol. Lett. 19, 554–563.
Geng, X., Li, K., 2002. Degradation of non-phenolic lignin by the white-rot fungus Pycnoporus cinnabarinus. Appl. Microbiol. Biot. 60, 342–346.
Gill, S.R., Pop, M., DeBoy, R.T., Eckburg, P.B., Turnbaugh, P.J., Samuel, B.S., Gordon, J.I., Relman, D.A., Fraser-Liggett, C.M., Nelson, K.E., 2006. Metagenomic analysis of the human distal gut microbiome. Science 312, 1355–1359.
Gutierrez, T., Green, D.H., Nichols, P.D., Whitman, W.B., Semple, K.T., Aitken, M.D., 2013. *Polycyclovorans algicola* gen. nov., sp. nov., an aromatic-hydrocarbon-degrading marine bacterium found associated with laboratory cultures of marine phytoplankton. Appl. Environ. Microb. 79, 205–214.
Hardin, G., 1960. The competitive exclusion principle. Science 131, 1292–1297.
Hilscher, A., Knicker, H., 2011. Carbon and nitrogen degradation on molecular scale of grass-derived pyrogenic organic material during 28 months of incubation in soil. Soil Biol. Biochem. 43, 261–270.
Jacquiod, S., Franqueville, L., Cécillon, S., Vogel, T.M., Simonet, P., 2013. Soil bacterial community shifts after chitin enrichment: an integrative metagenomic approach. PLoS One 8, e79699.
Kögel-Knabner, I., 2002. The macromolecular organic composition of plant and microbial residues as inputs to soil organic matter. Soil Biol. Biochem. 34, 139–162.
Kõljalg, U., Nilsson, R.H., Abarenkov, K., Tedersoo, L., Taylor, A.F.S., Bahram, M., Bates, S.T., Bruns, T.D., Bengtsson-Palme, J., Callaghan, T.M., Douglas, B., Drenkhan, T., Eberhardt, U., Duenas, M., Grebenc, T., Griffith, G.W., Hartmann, M., Kirk, P.M., Kohout, P., Larsson, E., Lindahl, B.D., Luecking, R., Martin, M.P., Matheny, P.B., Nguyen, N.H., Niskanen, T., Oja, J., Peay, K.G., Peintner, U., Peterson, M., Poldmaa, K., Saag, L., Saar, I., Schuessler, A., Scott, J.A., Senes, C., Smith, M.E., Suija, A., Taylor, D.L., Telleria, M.T., Weiss, M., Larsson, K.H., 2013. Towards a unified paradigm for sequence-based identification of fungi. Mol. Ecol. 22, 5271–5277.
Kubartová, A., Ranger, J., Berthelin, J., Beguiristain, T., 2009. Diversity and decomposing ability of saprophytic fungi from temperate forest litter. Microb. Ecol. 58, 98–107.
Lee, L.H., Azman, A.S., Zainal, N., Eng, S.K., Ab Mutalib, N.S., Yin, W.F., Chan, K.G., 2014. *Microbacterium mangrovi* sp. nov., an amylolytic actinobacterium isolated from mangrove forest soil. Int. J. Syst. Evol. Microb. 64, 3513–3519.
Li, Y., Chen, N., Harmon, M.E., Li, Y., Cao, X., Chappell, M.A., Mao, J., 2015. Plant species rather than climate greatly alters the temporal pattern of litter chemical composition during long-term decomposition. Sci. Rep. 5, 15783.
Li, D., Li, Z., Zhao, B., Zhang, J., 2020. Relationship between the chemical structure of straw and composition of main microbial groups during the decomposition of wheat and maize straws as affected by soil texture. Biol. Fertil. Soils 56, 11–24.
Liu, D., Keiblinger, I.M., Leitner, S., Mentler, A., Zechmeister-Boltenstem, S., 2016. Is there a convergence of deciduous leaf litter stoichiometry, biochemistry and microbial population during decay? Geoderma 272, 93–100.
Lladó, S., Žifčáková, L., Větrovský, T., Eichlerová, I., Baldrian, P., 2016. Functional screening of abundant bacteria from acidic forest soil indicates the metabolic potential of Acidobacteria subdivision 1 for polysaccharide decomposition. Biol. Fertil. Soils 52, 251–260.
Maarastawi, S.A., Frindte, K., Geer, R., Krober, E., Knief, C., 2018. Temporal dynamics and compartment specific rice straw degradation in bulk soil and the rhizosphere of maize. Soil Biol. Biochem. 127, 200–212.
Manickam, N., Mau, M., Schlömann, M., 2006. Characterization of the novel HCH-degrading strain, *Microbacterium* sp. ITRC1. Appl. Microbiol. Biotechnol. 69, 580–588.
Mao, J.D., Schmidt-Rohr, K., 2004. Accurate quantification of aromaticity and nonprotonated aromatic carbon fraction in natural organic matter by ^{13}C solid-state nuclear magnetic resonance. Environ. Sci. Technol. 38, 2680–2684.
Martins, L.F., Antunes, L.P., Pascon, R.C., de Oliveira, J.C., Digiampietri, L.A., Barbosa, D., Peixoto, B.M., Vallim, M.A., Viana-Niero, C., Ostroski, E.H., Telles, G.P., Dias, Z., da Cruz, J.B., Juliano, L., Verjovski-Almeida, S., da Silva, A.M., Setubal, J.C., 2013. Metagenomic analysis of a tropical composting operation at the sao paulo zoo park reveals diversity of biomass degradation functions and organisms. PLoS One 8, e61928.
Moitinho, M.A., Bononi, L., Souza, D.T., Melo, I.S., Taketani, R.G., 2018. Bacterial succession decreases network complexity during plant material decomposition in mangroves. Microb. Ecol. 76, 954–963.
Mula-Michel, H.P., Williams, M.A., 2013. Soil type modestly impacts bacterial community succession associated with decomposing grass detrituspheres. Soil Sci. Soc. Am. J. 77, 133–144.
Olsen, S.R., Cole, C.V., Watanabe, F.S., Dean, L.A., 1954. Estimation of available phosphorus in soils by extraction with sodium bicarbonate. In: USDA Circ. No. 939. USDA, Washington, DC, pp. 1–19.
Park, M.J., Kim, M.K., Kim, H.B., Im, W.T., Yi, T.H., Kim, S.Y., Soung, N.K., Yang, D.C., 2008. *Microbacterium ginsengisoli* sp. nov., a β-glucosidase-producing bacterium isolated from soil of a ginseng field. Int. J. Syst. Evol. Microb. 58, 429–433.
Parsons, S.A., Congdon, R.A., Lawler, I.R., 2014. Determinants of the pathways of litter chemical decomposition in a tropical region. New Phytol. 203, 873–882.
Preston, C.M., Nault, J.R., Trofymow, J.A., 2009. Chemical changes during 6 years of decomposition of 11 litters in some Canadian forest sites. Part 2. ^{13}C abundance, solid-state ^{13}C NMR spectroscopy and the meaning of "lignin". Ecosystems 12, 1078–1102.
Purahong, W., Wubet, T., Lentendu, G., Schloter, M., Pecyna, M.J., Kapturska, D., Hofrichter, M., Krüger, D., Buscot, F., 2016. Life in leaf litter: novel insights into community dynamics of bacteria and fungi during litter decomposition. Mol. Ecol. 25, 4059–4074.
Rime, T., Hartmann, M., Stierli, B., Anesio, A.M., Frey, B., 2016. Assimilation of microbial and plant carbon by active prokaryotic and fungal populations in glacial forefields. Soil Biol. Biochem. 98, 30–41.
Senechkin, I.V., Speksnijder, A.G.C.L., Semenov, A.M., van Bruggen, A.H.C., van Overbeek, L.S., 2010. Isolation and partial characterization of bacterial strains on low organic carbon medium from soils fertilized with different organic amendments. Microb. Ecol. 60, 829–839.
Siciliano, S.D., Palmer, A.S., Winsley, T., Lamb, E., Bissett, A., Brown, M.V., van Dorst, J., Ji, M.K., Ferrari, B.C., Grogan, P., Chu, H.Y., Snape, I., 2014. Soil fertility is associated with fungal and bacterial richness, whereas pH is associated with community composition in polar soil microbial communities. Soil Biol. Biochem. 78, 10–20.
Šnajdr, J., Cajthaml, T., Valášková, V., Merhautová, V., Petránková, M., Spetz, P., Leppänen, K., Baldrian, P., 2011. Transformation of *Quercus petraea* litter: successive changes in litter chemistry are reflected in differential enzyme activity and changes in the microbial community composition. FEMS Microbiol. Ecol. 75, 291–303.
Voříšková, J., Baldrian, P., 2013. Fungal community on decomposing leaf litter undergoes rapid successional changes. ISME J. 7, 477–486.
Wallenstein, M.D., Haddix, M.L., Ayres, E., Steltzer, H., Magrini-Bair, K.A., Paul, E.A., 2013. Litter chemistry changes more rapidly when decomposed at home but converges during decomposition-transformation. Soil Biol. Biochem. 57, 311–319.
Wang, X.Y., Sun, B., Mao, J.D., Sui, Y.Y., Cao, X.Y., 2012. Structural convergence of maize and wheat straw during two-year decomposition under different climate conditions. Environ. Sci. Technol. 46, 7159–7165.
Weber, C.F., King, G.M., Aho, K., 2015. Relative abundance of and composition within fungal orders differ between cheatgrass (*Bromus tectorum*) and sagebrush (*Artemisia tridentata*)-associated soils. PLoS One 10, e0117026.
Wickings, K., Grandy, A.S., Reed, S., Cleveland, C., 2011. Management intensity alters decomposition via biological pathways. Biogeochemistry 104, 365–379.
Wickings, K., Grandy, A.S., Reed, S.C., Cleveland, C.C., 2012. The origin of litter chemical complexity during decomposition. Ecol. Lett. 15, 1180–1188.
Xia, M., Zhao, B.Z., Xiying, H., Zhang, J.B., 2015. Soil quality in relation to agricultural production in the North China Plain. Pedosphere 25, 592–604.
Zech, W., Senesi, N., Guggenberger, G., Kaiser, K., Lehmann, J., Miano, T.M., Miltner, A., Schroth, G., 1997. Factors controlling humification and mineralization of soil organic matter in the tropics. Geoderma 79, 117–161.
Zhang, Z.J., Li, H.Y., Hu, J., Li, X., He, Q., Tian, G.M., Wang, H., Wang, S.Y., Wang, B., 2015. Do microorganism stoichiometric alterations affect carbon sequestration in paddy soil subjected to phosphorus input? Ecol. Appl. 25, 866–879.